Rubberized reinforced concrete columns under axial and cyclic loading

Heba A. Mohamed, Hilal Hassan, Mahmoud Zaghlal
Structural Engineering Dept., Faculty of Engineering, Zagazig University, Zagazig, Egypt
hebawahbe@yahoo.com, http://orcid.org/0000-0002-8292-720X
hilalcivil@yahoo.com , http://orcid.org/0000-0001-5486-5497
eng_m_z@yahoo.com , http://orcid.org/0000-0003-2579-6132

Mohammed A. M. Ahmed
High Institute of Engineering and Technology, Arish, Egypt
eng.mohamed.atef@Sinaieng.edu.eg, http://orcid.org/0009-0002-4033-6855

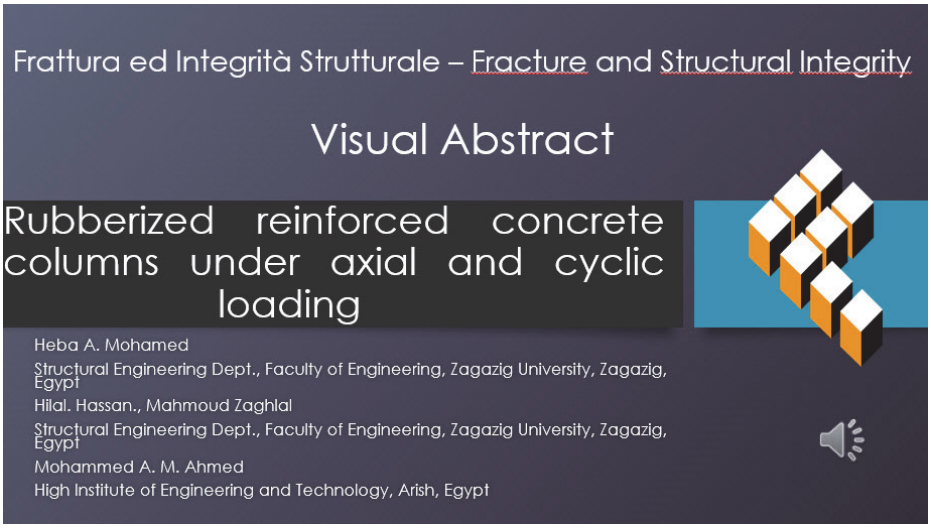

Citation: Heba, M., Hassan, H., Zaghlal, M., Ahmed, M., Performance of rubberized reinforced concrete columns under axial and cyclic loading, Frattura ed Integrità Strutturale, 70 (2024) 286-309.

Received: 16.07.2024
Accepted: 15.09.2024
Published: 21.09.2024
Issue: 10.2024

KEYWORDS. Rubberized reinforced concrete, Axial loads, Cyclic loading, RC columns, Finite element, Crumb rubber.

INTRODUCTION

Rubber waste is a highly flexible material that endures most environmental conditions. Rubber concrete, a new concrete that is made from rubber tire crumbs instead of aggregates, has been developed effectively. Earlier investigations have demonstrated that the ductility, toughness, energy absorption, and damping ratio of concrete were all enhanced by adding rubber to the concrete's aggregates [1]. However, earlier research also showed that using rubber to replace normal particles decreased rubberized concrete's structural strength [2]. The reduction in these characteristics depends on numerous variables, including the amount of rubber replaced, the substitution of fine or coarse aggreates, and

the usage of any additional cementation material, like silica fume. To increase the mechanical qualities of rubberized concrete, such as its modulus of elasticity, compressive strength, and axial flexural strength, Elchalakani [3] suggested adding silica fume to the mixture. Youssf et al. [4] considered the consequences of adding FRP to Crumb Rubber Concrete (CRC) to reduce the disadvantages of partially substituting discarded waste rubber tires with concrete aggregate. The results demonstrate that the usage of FRP essentially lowers the strength loss while preserving the advantages of rubberized concrete's increased flexibility.

Very few searches using larger structural components composed of CRC have been conducted. There is no agreement among researchers regarding how applying CRC affects the structural performance of structural elements, hence the findings of these studies are contradictory [5]. Son et al. [6] examined the effectiveness of utilizing crump rubber concrete to enhance the energy absorption and deformability of RC columns subjected to only axial loads. Tests were conducted on six 200 mm × 300 mm × 1600 mm column specimens. The factors that were examined in this experimental investigation were the rubber content (2.7 and 5.4% by total aggregate volume), the concrete's compressive strength (24 and 28 Mpa), and the diameters of the rubber particles (0.6 and 1.0 mm). The results of the test demonstrated that the curvature ductility of the tested column increased from 45% to 90%, based on the rubber's content and size.

Current design codes for new construction describe the seismic details for reinforced concrete columns, such as ACI [7], to achieve their codified target seismic performance [8]. Previous research has experimentally and analytically verified these seismic details, demonstrating how stringent seismic design recommendations for RC columns can improve their deformation capabilities [9], which in turn improves the seismic performance of structures. Traditionally, scientists have concentrated on the damage and nonlinear properties of materials for concrete. The material's capacity to take in some of the work of the external force as internal energy serves as the foundation for damping, a crucial dynamic property for the structure when subjected to earthquake and vibration activity [10]. This process will inevitably result in some material degradation. The capacity of the material to absorb some of the external force work and generate permanent structural deformation is known as plastic deformation, or the intrinsic deformation of concrete when exposed to external load [11]. This deformation will undoubtedly cause some material damage. As a result, it is feasible to calculate the concrete material's damage under cyclic loads since the aggregate energy consumption of material damage is the energy dissipation of the material under cyclic loads due to plastic deformation and the damping effect. Some research [12]signifies that incorporating rubber particles may significantly enhance the damping performance of concrete by improving the material's internal pore structure, increasing friction loss at the aggregate interface, and exhibiting viscoelastic qualities. Therefore, more attention from scientists studying material damping should be focused on how structural damage to rubber concrete accumulates under cyclical load. Most of the time, research revealed that utilizing rubber from old tires in concrete decreased its modulus of elasticity, and compressive strength when contrast to regular concrete. [13]. There aren't many studies on the behavior of RRC columns during earthquakes. Elghazouli et al. [14] studied the behavior of RRC under cyclic conditions. The study found that using recycled rubber particles instead of mineral aggregate enhanced the hysteretic damping ratio and energy dissipation. This was true even when the total amount of mineral aggregate remained unchanged. Furthermore, the material's flexural and compressive toughness, as well as its hysteretic curve and ductility, were found to have enhanced significantly. According to earlier studies, replacing the fine aggregate in concrete with CR can lessen the negative environmental effects of this material. Thus, the primary the purpose of this research is to ascertain the efficiency of using CR on the behavior and load capacity of RC columns at cyclic loading. In this research, the percentages of 0%, 10%, and 15% of the fine aggregate are substituted with the CR. Additionally, an experimental test is conducted to determine the influence of CR on the performance of circular and square RCC. At last, the capability of simulating rubberized concrete columns under cyclic loads using finite element analysis.

EXPERIMENTAL PROGRAM

Under an axial load, twelve reinforced concrete columns were tested. A study through experimentation was done on the influence of column height, cross-section, and the usage of crumb rubber on column capacity.

Specimen details

The experimental program was set up for two groups of column specimens. The first group of six circular columns made of reinforced concrete were 250 mm in diameter and 1500 mm and 1800 mm in height, respectively. In the second group, six square column sections with the same width (250 mm) and height were designed. All columns were braced columns in a hinged case. The tested columns' dimensions and reinforcement (RFT) were chosen according to Egyptian code (ECP

203/2010) for the design and construction of concrete structures. Each tested column was reinforced with six bars with a 12 mm diameter and yield stress of 550 MPa and tensile strength of 640 MPa. Stirrups of 8 mm diameter were employed with a yield stress of 280 MPa. In each column specimen, there was a 25 mm clear concrete cover. One column for each group was designed as a control specimen without any crump rubber, and two more columns were designed with replacement fine aggregates of crump rubber at 10% and 15%, respectively. Fig. 1 display the details of RFT and dimensions of the column specimens, and Table 1 contains the titles and specifics of the RC columns that have been tested. The code of specimen in this table starts with "R0%" stands for traditional concrete or "R10%" and "R10%" for CRC. This is followed by "H1.5" or "H1.8" to indicate the specimen's height. The cross-section of the specimens is indicated by the letter's "S" for square and "C" for circular.

Casting, mix percentages, and material specifications

For this study, three distinct blends of concrete (M1, M2, and M3) were selected according to replacement by volume of the fine aggregate by varying percentages of CR (0%, 10%, and 15%), respectively. The mix design was created in compliance with ECP 203. The proportion of cement and the ratio of water to cement (W/C) were 350 kg/m3 and 0.5, respectively. Table 2 displays the mix percentages for the three mixtures. The concrete's tensile and compressive strengths were measured using standard cylinders (150 mm diameter, 300 mm height) and cubes (180 mm in size). Middle-sized sand with a specific gravity of 2.54 and a fineness modulus of 2.69 was used as fine aggregate, while coarse aggregates with a nominal maximum size of 38 mm and a specific gravity of 2.78 were used as coarse aggregate for all mixes. Tire rubber waste was mechanically ground to produce CR with a specific gravity of 0.95. As shown in Fig 2, two different sizes of CR were blended at a ratio of 1:1 [15] for the current research. Fig. 3 displays the results of the sieve analysis of the CR, fine aggregate, and coarse aggregate utilized in this investigation. The results display a 78 mm slump value in normal concrete (M1). For rubberized concrete with a 10% crumb rubber (M2) and a 15% crumb rubber (M3), the values were 67 and 63 mm, respectively.

Specimen code	%Crumb rubber	Height (mm)	Boundary conditions $(\lambda)=\frac{(k.H_0)}{(b\ or\ D)}$ Hinged- Hinged (Braced) (K=1)	Cross section	Reinforcement
R0%H1.5C	0%	1500	(λ) = 6	Circular (D=250mm)	As = 6ϕ12
R10%H1.5C	10%	1500	(λ) = 6		
R15%H1.5C	15%	1500	(λ) = 6		
R0%H1.8C	0%	1800	(λ) = 7.2		
R10%H1.8C	10%	1800	(λ) = 7.2		
R15%H1.8C	15%	1800	(λ) = 7.2		
R0%H1.5S	0%	1500	(λ) = 6	Square (250*250mm)	
R10%H1.5S	10%	1500	(λ) = 6		
R15%H1.5S	15%	1500	(λ) = 6		
R0%H1.8S	0%	1800	(λ) = 7.2		
R10%H1.8S	10%	1800	(λ) = 7.2		
R15%H1.8S	15%	1800	(λ) = 7.2		

Table 1: The test specimens' specifics.

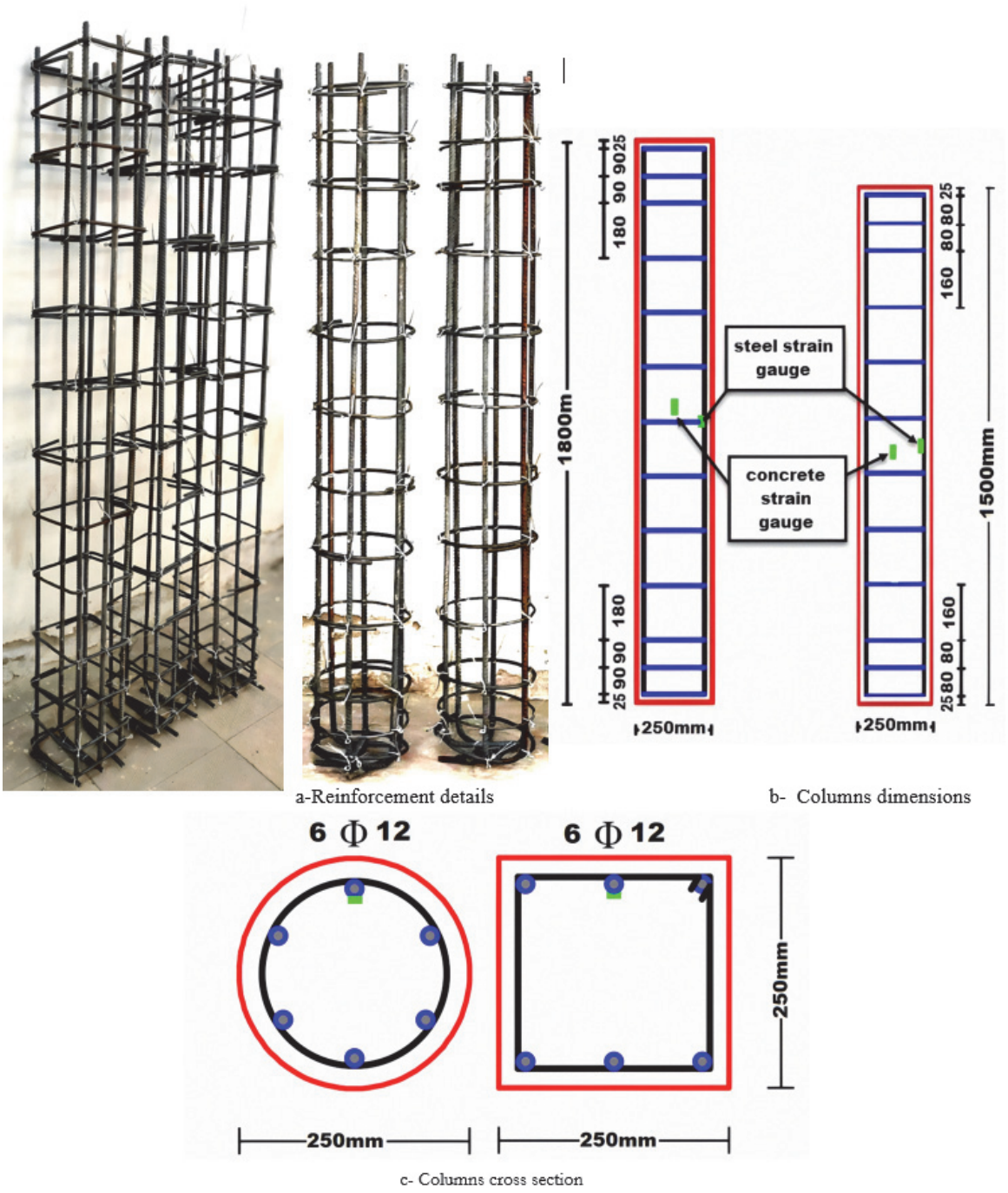

Figure 1: Columns cross section, dimensions, and reinforcement details.

Constituents	M1 (R0%)	M2 (R10%)	M3 (R15%)
Cement (kg/ m^3)	350	350	350
Coarse aggregate (kg/ m^3)	1129	1129	1129
Fine aggregate (kg/ m^3)	752	724	710
W/C	0.5	0.5	0.5
Crumb rubber (kg/ m^3)	--	28	42

Table 2: Concrete mix proportions.

a- particles (0.6 – 1.8 mm)

b- particle (1.8 - 6 mm)

Figure 2: Particles crump rubber.

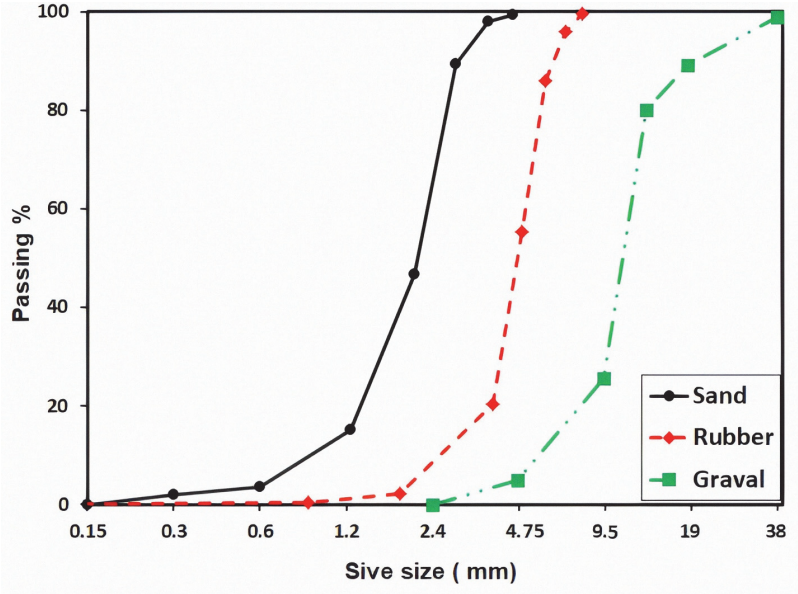

Figure 3: Sieve analysis results.

Instrumentation and test setup

The columns were subjected to an axial compression force throughout the test. A 2800 kN capacity testing machine was used to inspect every column. For every column, an axial load was applied until it failed. To spread the axial load, a stiff steel plate was positioned at the top and bottom of every column specimen. Two linearly variable transformers (LVDTs) were used to calculate the vertical displacement, as shown in Fig. 4. At the end of loading, a calibrated load cell was used for an instant measurement of the axial force. Using a data logger, the displacement readings and loads were recorded. Also, the strain in concrete and steel was measured by concrete strain and steel strain gauges, respectively. A load increment equal to 0.1 of the expected ultimate load was applied up to failure. As shown in Fig. 4, hinge support along the x-axis was supplied at both ends of the columns.

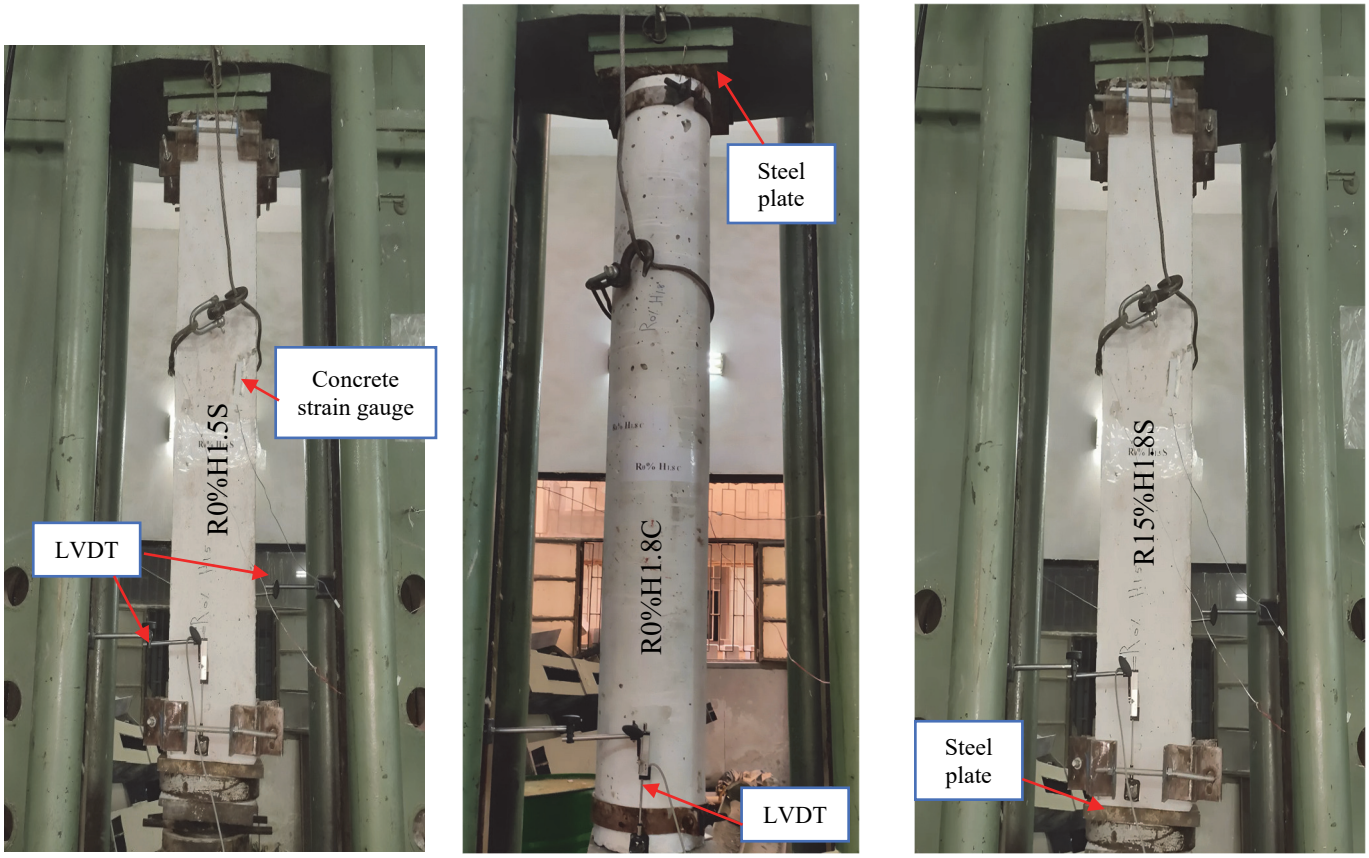

Figure 4: Test apparatus and setup.

TEST RESULTS AND DISCUSSION

Concrete's mechanical characteristics

Fig. 5 illustrates the effects of CR on the compressive strength (Fcu) of concrete. When 10% CR added to the fine aggregate, the Fcu value dropped from 30 MPa to 24.5 MPa by 18.33% when compared to the specimens without CR. Furthermore, the value of Fcu dropped by 26.5% when contrasted with concrete devoid of crumb rubber when the proportion of CR was rised to 15% of fine aggregate. The noticed decrease in Fcu may be due to CR's very poor strength and stiffness. In addition, raising the CR with tiny particles might cause voids in concrete. Also, it was found that when fine aggregate was added at 10% and 15%, the tensile strength (Ftu) of the concrete specimens dropped. In a comparison between concrete specimens without CR and specimens cast with a 10% replacement ratio of CR, the tensile strength (Ftu) drop was 18.5%; however, the decrease in tensile strength reached 25.5% when the when the ratio of CR was raised to 15%. This indicated that the impact of fine particles acting as voids may be mitigated by the large rubber fibers in concrete with a CR of 10%, but that the influence could increase in concrete with a CR of 15% due to fine crumb rubber particles serving as voids. The modulus of elasticity, tensile strength, and compressive strength reduced when the proportion of CR in concrete increased, according to previous studies [16].

Load capacity

The findings of the experiments of the examined RC columns are shown in Table 3. The specimen code is displayed in the first column, followed by the ultimate load (Pu) and the displacement at yield (Δy) and ultimate displacement (Δu) in the second and third columns. The final column also included the ductility index (DI) for each of the columns.

After adding 10% and 15% crumb rubber, respectively, to rubberized reinforced concrete columns, the ultimate load for circular RC column specimens measuring 1500 mm in height dropped from 1611 kN to 1370 kN and 1285 kN by 14.95% and 20.24%. When rubberized concrete was used as a 10% and 15% replacement for fine aggregate, respectively, the ultimate load was reduced from 1600 kN to 1389 kN and 1280 kN by 13.19% and 20% at the circular cross section with a height of 1800 mm when compared to reinforced concrete columns without crumb rubber.

Fig. (6) c illustrates that the ultimate load for square cross-section column specimens with a height of 1500 mm dropped from 1880kN to 1639kN and 1477kN for rubberized reinforced concrete columns with 10% and 15% crumb rubber, respectively, by 12.82% and 21.44%. In comparison to reinforced concrete columns without crumb rubber (case of square column with 1800 mm), the ultimate load was decreased from 1850 kN to 1575 kN and to 1450 kN by 14.86% and 21.62% when replacing fine aggregate by 10% and 15%, respectively, with CR. This was due to the inadequate bonding of the rubber and the cement as well as the partial replacement of crumb rubber for the aggregates[17]. Fig. 6 shows the relationship between displacement values and experimentally measured loads.

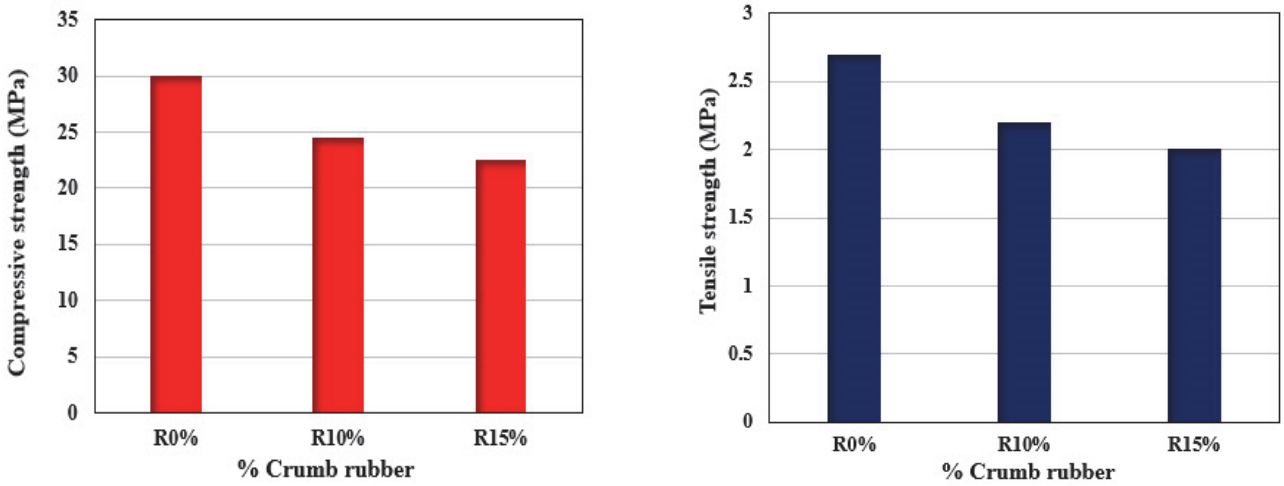

a- Compressive strength b- Tensile strength

Figure 5: Effects of CR on the characteristics of concrete.

Specimen code	P_u (kN)	Δy (mm)	Δu (mm)	DI
R0%H1.5C	1611	3.37	6.45	1.91
R10%H1.5C	1370	3.6	6.65	1.84
R15%H1.5C	1285	3.69	6.54	1.77
R0%H1.8C	1600	3.9	5.95	1.53
R10%H1.8C	1389	4	5.85	1.46
R15%H1.8C	1280	4.2	5.55	1.32
R0%H1.5S	1880	3.36	5.8	1.73
R10%H1.5S	1639	3.57	5.8	1.62
R15%H1.5S	1477	3.7	5.75	1.56
R0%H1.8S	1850	3.65	6.34	1.74
R10%H1.8S	1575	4	6.2	1.55
R15%H1.8S	1450	3.95	6	1.52

Table 3: Experimental results of specimens

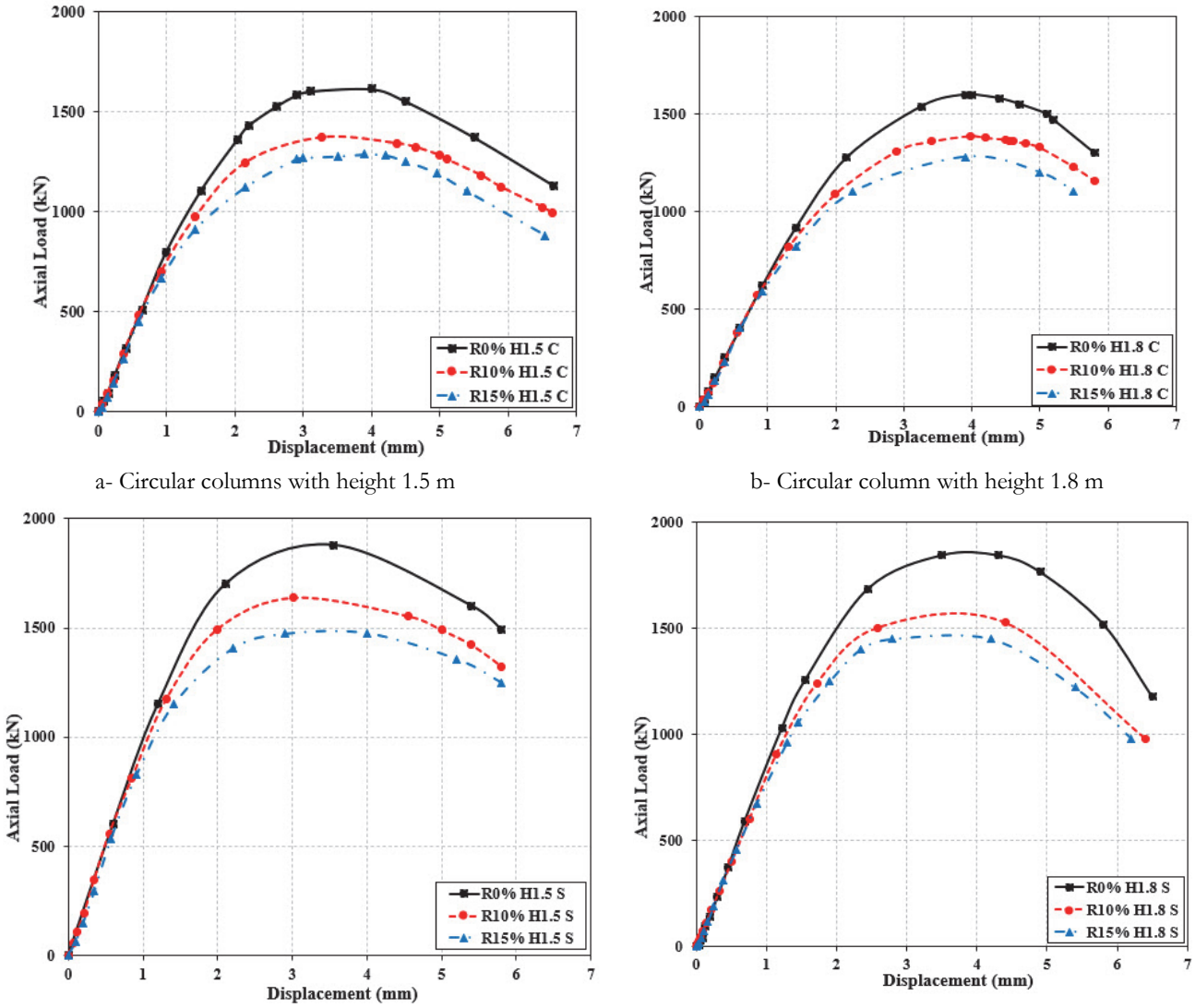

a- Circular columns with height 1.5 m

b- Circular column with height 1.8 m

c- Square columns with height 1.5 m

d- Square columns with height 1.8 m

Figure 6: Load – displacement of specimens.

Failure modes and fracture patterns

Every column was exposed to axial loads till failure. The failure pattern of RRC columns was observed to be quite different from that of RC columns. Figs. 7-9 depicts the modes of failure for all tested columns. It is evident that most of the tested columns had fine cracks that began below the column height and gradually expanded quietly and uniformly to the center of the column. Unlike the rubberized reinforced concrete column, which had a massive crack, all the RC columns had tiny cracks separated by short spaces. Fig. 7 illustrates how the crack's width expanded in direct proportion to the applied force, becoming evident at the failure load in the RC specimen. The crushing degradation grade increased as the applied force increased for rubberized reinforced concrete columns with 10% CR. This results in a significant volume of air bubbles and poor workability because of a huge quantity of CR that could not spread evenly throughout the mix[18]. As seen in Fig. 8,this specimen also displayed longitudinal steel bar buckling. In Fig. 8(a), splitting failure in the central zone of the specimen (R10%H1.5S) was attributed to the progression of vertical cracks; no steel bar buckling was seen in this instance. The development of vertical cracks in the central zone of the rubberized concrete columns with a 15% CR replacement ratio resulted in a splitting failure pattern. These specimens showed notable steel bar buckling when the applied load approached the maximum capacity and, finally, collapsed in a high grade of crushing at the maximum load, as shown in Fig. 9. Finally, under axial loading, the RC columns are better in terms of load capacity and mode of failure at the loading termination than the rubberized concrete columns.

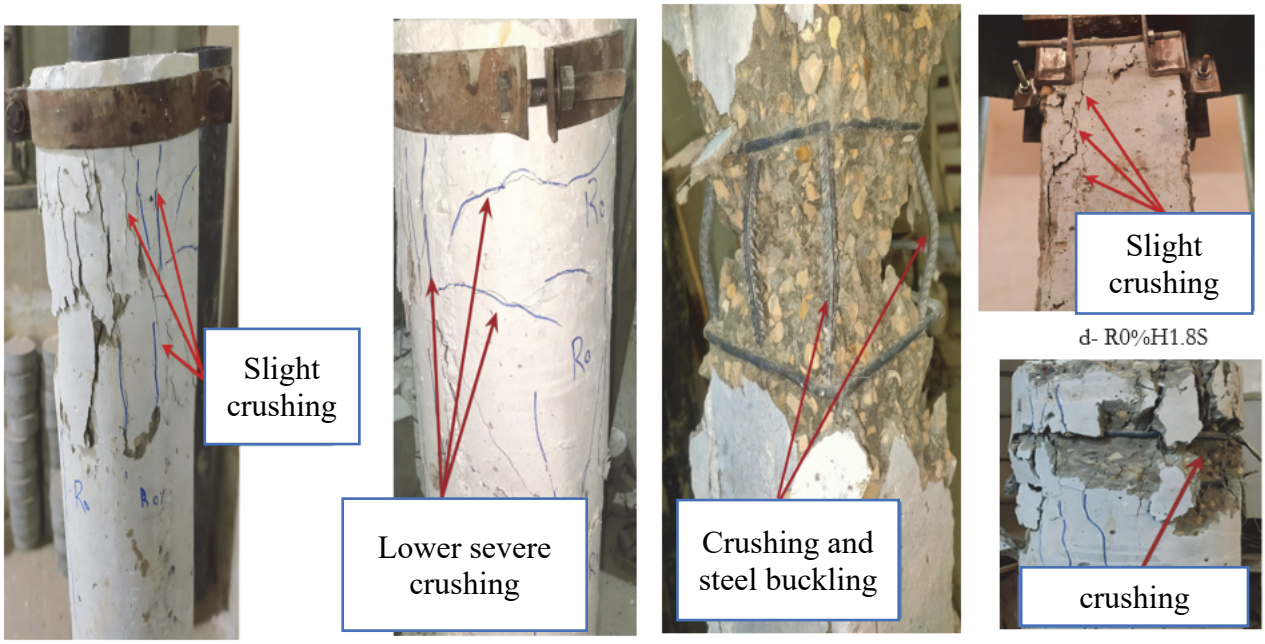

a- R0%H1.5C b- R0%H1.8C c- R0%H1.5S d- R0%H1.8S e- R0%H1.8C

Figure 7: Modes of failure of columns without CR.

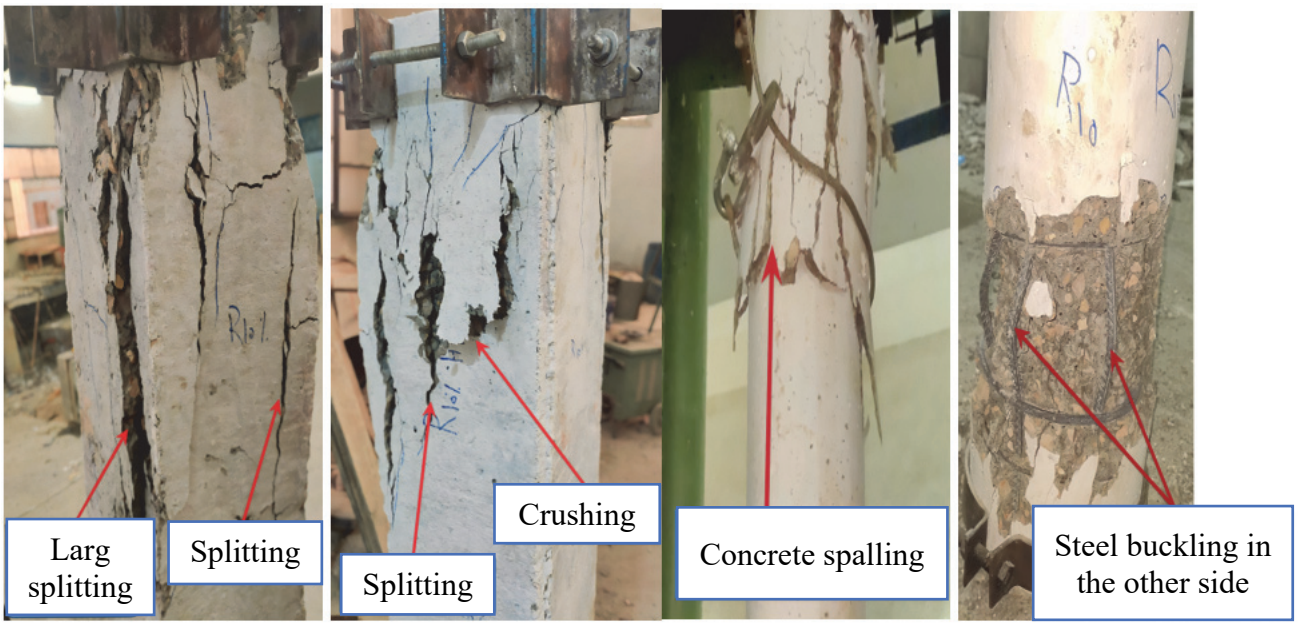

a-R10%H1.5S b- R10%H1.8S c- R0%H1.5C d- R0%H1.8C

Figure 8: Modes of failure of columns with 10% CR

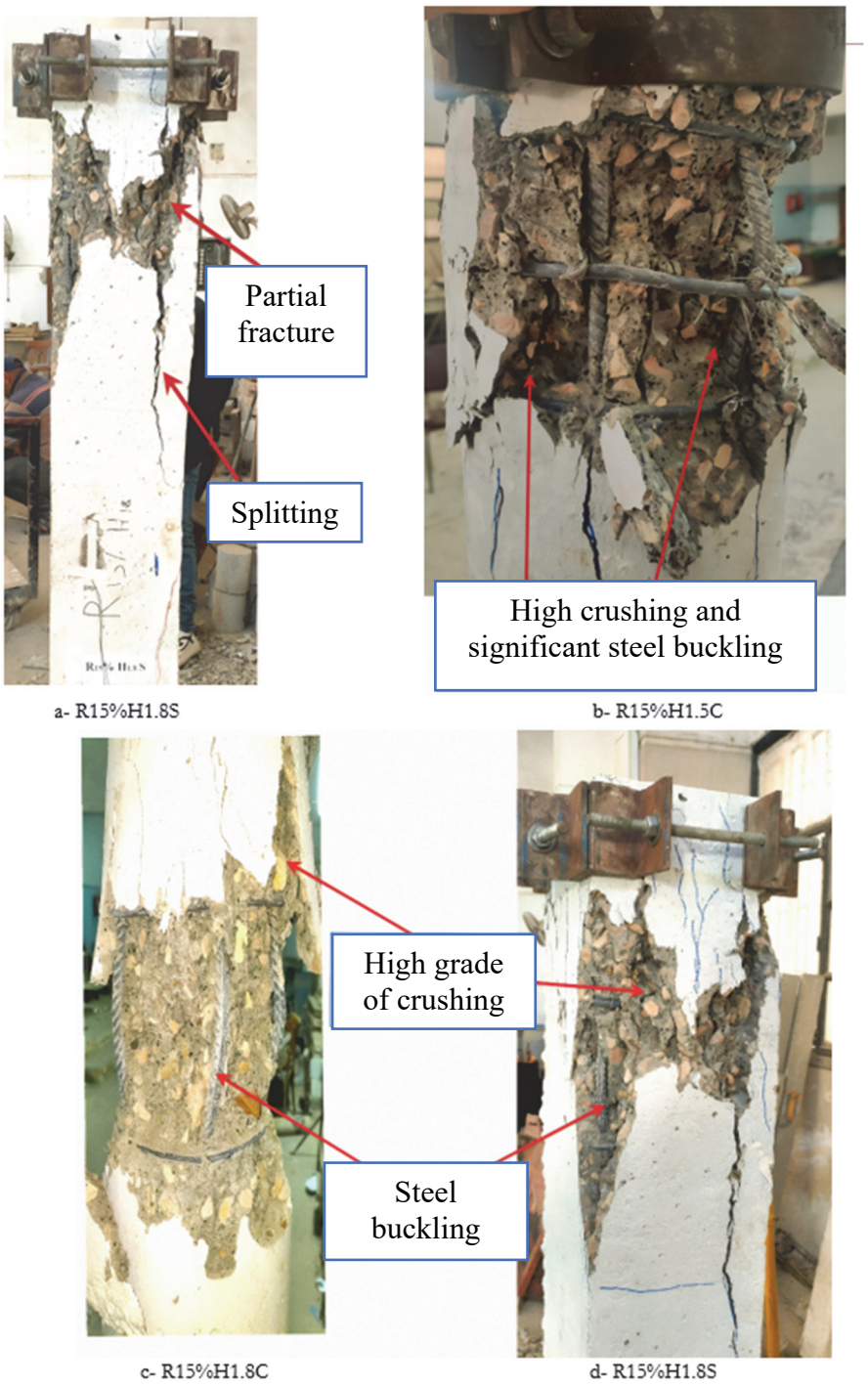

Figure 9: Modes of failure of columns with 15% CR.

Ductility

The capability of a structure's part to tolerate internal forces with high deformation is known as its ductility, and calculating the ductility value can provide a clear picture of the capacity for plastic deformation regarding column specimens. The proportion of the Δu of the RC columns to the Δy is defined as the ductility index (DI). Fig. 10 illustrates the ductility index decrease for each studied rubberized reinforced concrete column specimen, and Table 3 displays their data. The ductility index decreased as the CR ratio raised from 0% to 10%. Additionally, the ductility index was marginally lowered by an increase in the CR ratio from 10% to 15%. The decreasing was very significant in the instance of the rubberized reinforced concrete specimen with 15% of crumb rubber (R15%H1.8C), and medium in case of the specimen with 10% of crumb rubber (R10%H1.8C). The ductility index for the rubberized reinforced concrete specimens R15%H1.8C and R10%H1.8C

decreased by about 13.72% and 4.58% compared to the control concrete column (normal concrete), respectively. Therefore, in the case of 10% and 15% CR, the rate of decrease in the DI was computed by 10.92% and 12.64% for a square column with a height of 1800 mm (R10%H1.8S and R15%H1.8S) compared to a square column without CR (R0%H1.8S).

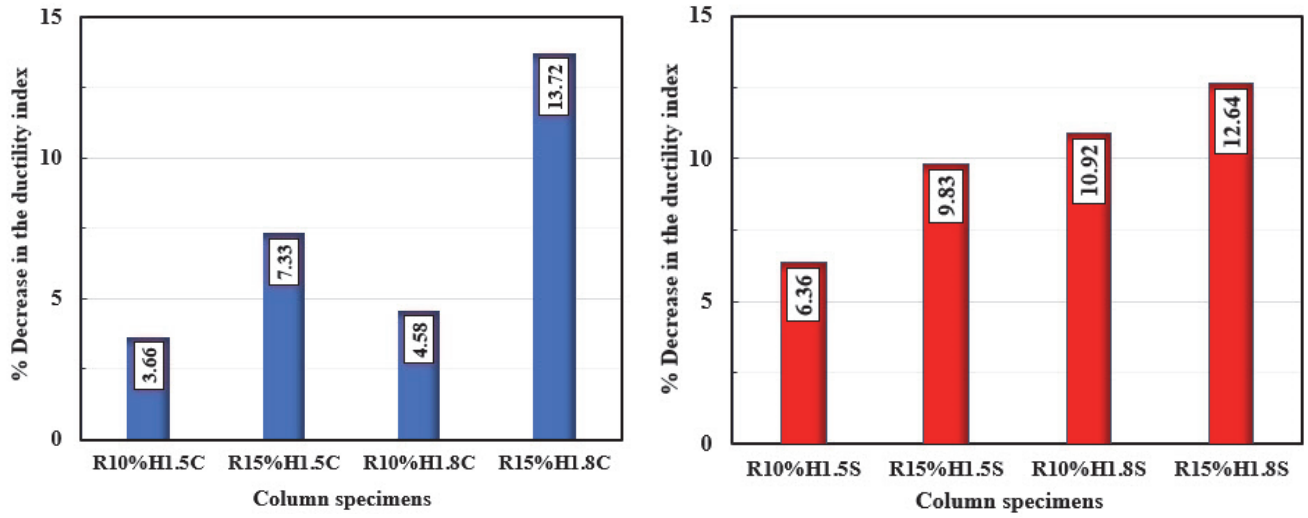

a- circular columns b- square columns

Figure 10: Percentage reduction in the RRC column specimens' ductility index when compared to the control column specimens.

FINITE ELEMENT MODELING

Model set-up

The finite element (FE) program ABAQUS/Standard [19] was used to model the behavior of rubberized reinforced concrete columns under cyclic loads. An FE model in three dimensions was created. To simulate steel bars and stirrups in the FE model, we used linear 3-D trusses elements with two nodes (T3D2). This element (T3D2) was used with structured meshes. An eight-node linear brick with reduced integration and hourglass control elements (C3D8R) was used to simulate concrete. The center of this element (C3D8R) is where the integration point is located. Small components are therefore needed to represent a stress concentration at a structure's boundary. Stresses and strains are most accurate at the integration points. It should be noted that ABAQUS and other programs use reduced-order integration, which makes it possible to calculate element matrices quickly and affordably. According to Fig. 11, the reinforcement was fully bonded and embedded in the concrete region. As seen in Fig. 12, the axial loading configuration and boundary condition were employed in the FE model as experimental testing.

Material models

The concrete damage plasticity (CDP) model in ABAQUS/Standard [19] was used to study normal concrete and rubberized concrete's triaxial constitutive behavior (see Fig.13).This damage model for concrete is based on continuum plasticity and suggests that the material would break under tensile cracking as well as compressive crushing. Represented in the effective stress space, the yield function based on the Von Mises equivalent stress and the hydrostatic stress, respectively. The constitutive models of concrete in compression and tension were calibrated using experimental data (Fig. 14(a, b)). A bi-linear stress-strain curve is used in Fig. 14(a, b) to model the uniaxial tensile behavior of concrete. After the maximum tensile strain was achieved, the stress decreased linearly to zero. Fig. 14(c) displays the simulation of the reinforcing steel bars and stirrups using a linearly elastic-plastic model. The volumetric plastic strain variations of the material are defined by the CDP model by considering a non-associated plastic potential flow rule. The Drucker-Prager hyperbolic function represents the plastic potential flow function (G), which is expressed differently from the yield function. For steel reinforcement, bi-linear elastoplastic behavior was adopted with an elastic modulus of 200 GPa and a Poisson's ratio of 0.3. After the longitudinal reinforcement and stirrups had yielded, linear strain hardening was considered, and the fracture of the rebar was estimated when the steel rebars achieved their maximum strength. At the final strain point, an enormous drop in stress was characteristic of reinforcement fracture.

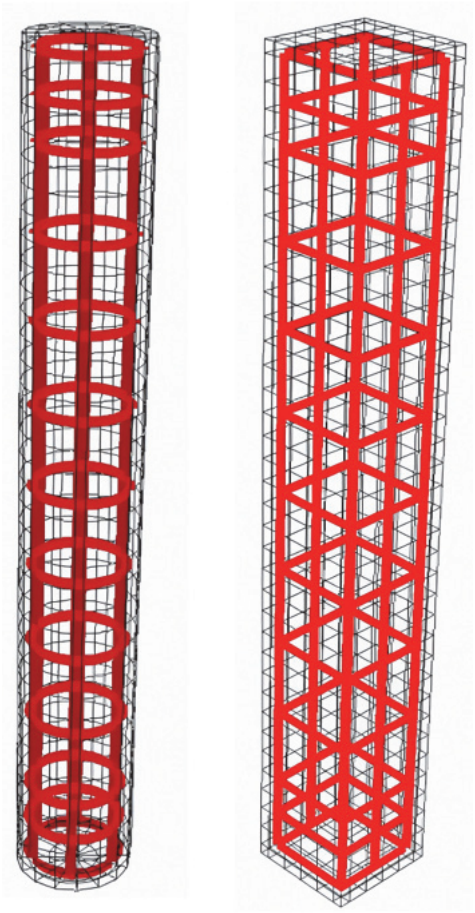

Figure 11. Finite element model

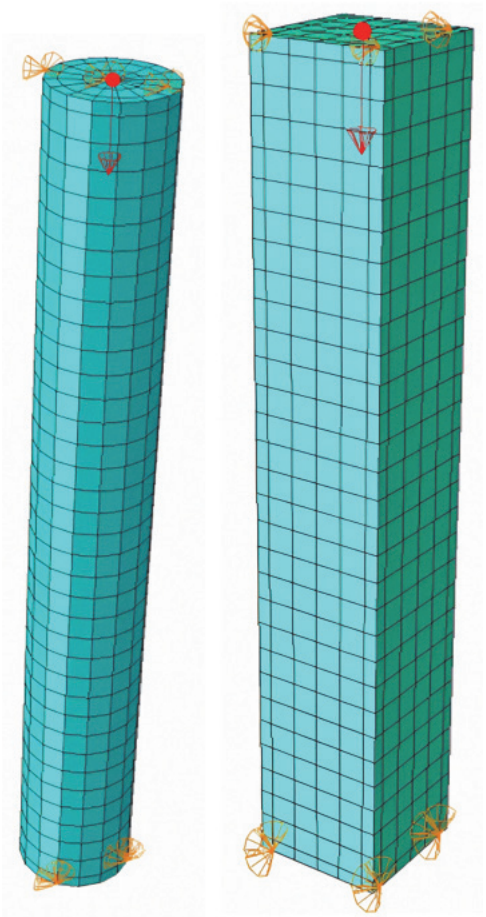

Figure 12. The FE model's boundary conditions and loads.

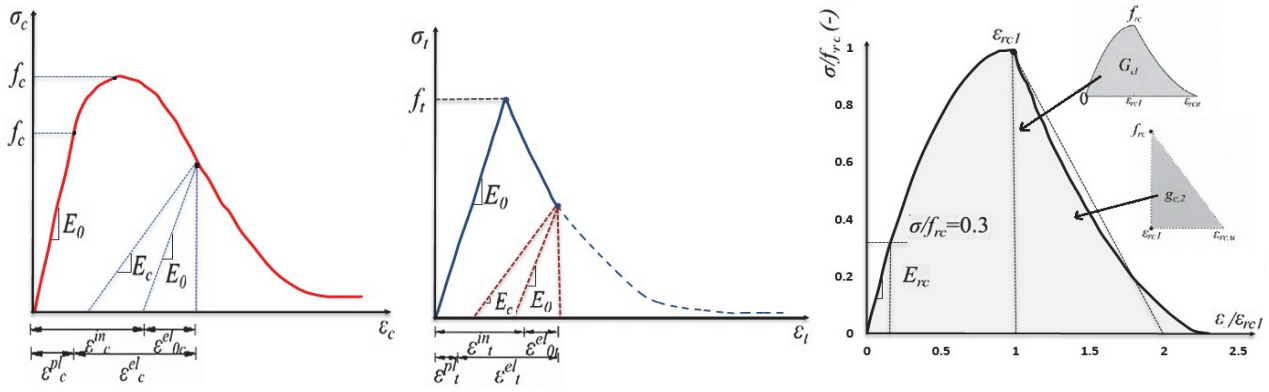

a- Compression b- Tension c- rubberized concrete

Figure 13. The plasticity model for concrete damage provided by ABAQUS [19].

FE validation

In terms of load-displacement curves, Figs. 15 and 16 present a comparison between experimental and finite element findings. All the specimens' FE findings revealed behaviors that were almost identical to those seen experimentally, although with a more noticeable deviation. The influence of the elements under investigation was almost identical to the experimental data, indicating that the FE model can accurately predict the performance of rubberized concrete columns with respect to their load capacity and mode of failure (Fig. 17). Table 4 illustrates the ultimate load and displacement at ultimate load dependent on the experimental and FEM results. With error values ranging from 2.56% to 5.5% for ultimate load and from 8.9% to 1.25% for displacement at ultimate load, the findings demonstrated a high concurrence between the experimental

and FEM analysis. One of the appropriate experiments that was done to simulate the rubberized concrete columns may be this numerical model.

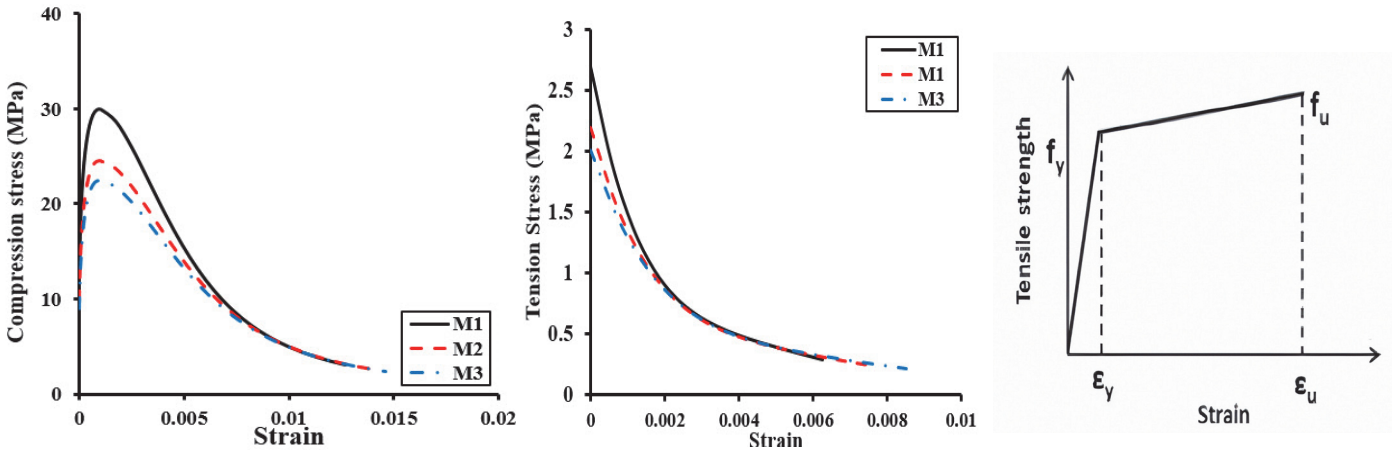

a- concrete compressive stress. b- concrete tension stress c- Steel

Figure 14. Models of constituent materials used in finite element analysis.

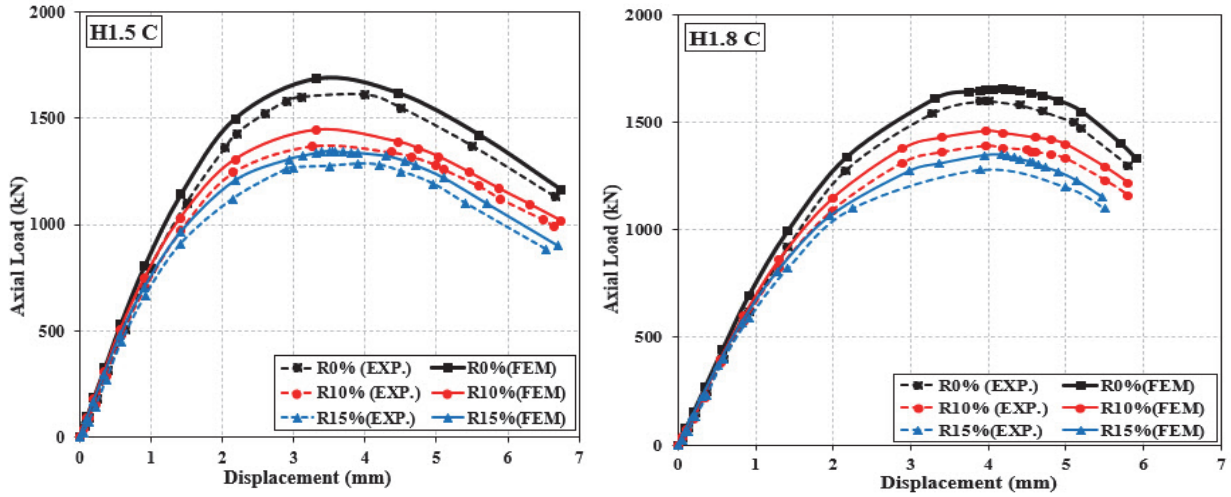

Figure 15. FE and experimental load-displacement curve comparison for circular columns.

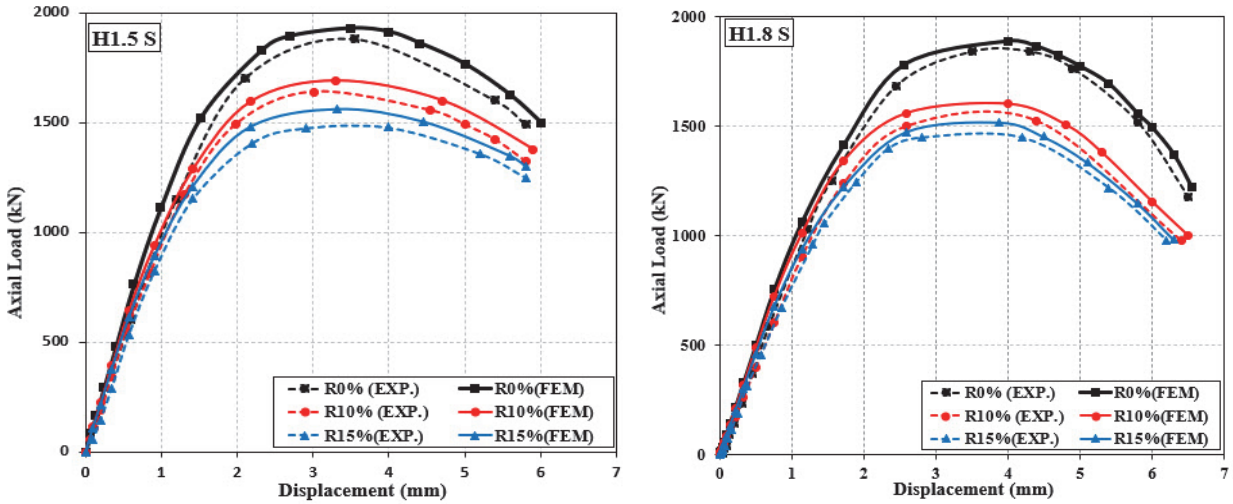

Figure 16 FE and experimental load-displacement curve comparison for square columns.

Specimen code	P_u (EXP.) (kN)	P_u (FEM.) (kN)	Error (%)	Displacement at ultimate load (EXP) (mm)	Displacement at ultimate load (FEM) (mm)	Error (%)
R0%H1.5C	1611	1686	4.65	3.5	3.2	8.5
R10%H1.5C	1370	1444	5.4	3.6	3.4	5.5
R15%H1.5C	1285	1345	4.66	3.9	3.55	8.9
R0%H1.8C	1600	1655	3.43	4	3.9	2.5
R10%H1.8C	1389	1458	5	3.9	4.1	5.12
R15%H1.8C	1280	1349	5.4	3.95	4.25	7.5
R0%H1.5S	1880	1927	2.5	3.55	3.4	4.2
R10%H1.5S	1639	1689	3	3.4	3.5	2.94
R15%H1.5S	1477	1559	5.5	3.8	3.65	3.95
R0%H1.8S	1850	1889	2.56	3.65	3.75	2.74
R10%H1.8S	1525	1603	5.11	4	3.9	2.5
R15%H1.8S	1450	1519	4.8	3.95	4	1.27

Table 4: Experimental vs. FEM results.

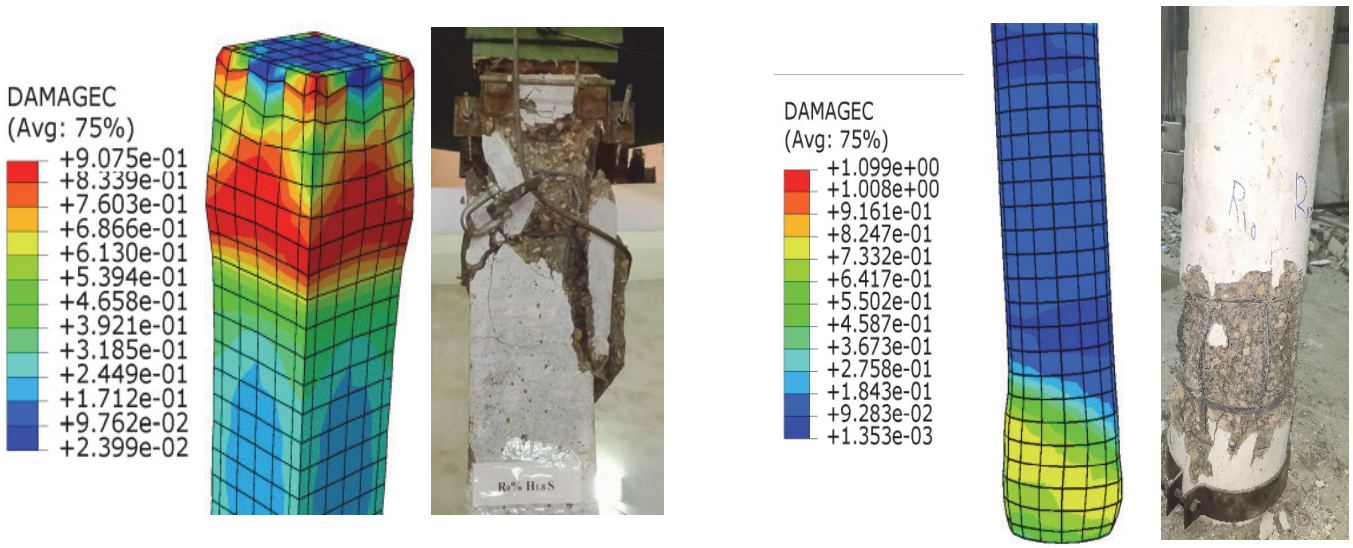

a- Square specimen (R0%H1.8S) b- Circular specimen (R10%H1.5C)

Figure 17. Crack patterns at column failure comparing experimental and finite element models.

FE verification Model (RC columns at cyclic loading)

A 3D nonlinear model of the RC columns tested by Hyeon Shin [20] in terms of geometry, material composition, and boundary conditions was presented. The square reinforced concrete column has a cross-sectional size of 600 mm by 600 mm and a height of 5050 mm, and the concrete cover is 70 mm thick. The main reinforcement is made of twenty longitudinally deformed rebars with a diameter of 19 mm. The employed stirrups were 13 mm in diameter and spaced 300 mm. In Fig. 18, the column specimen was placed between a top RC head measuring 1300 mm, 600 mm, and 700 mm and a bottom RC foundation measuring 1600 mm, 1500 mm, and 650 mm to replicate the fixed-end boundary condition. Rebar's nominal yield strength and concrete's nominal compressive strength are 400 MPa and 24 MPa, respectively. According to the loading technique described in ACI 374 [21], as seen in Fig. 19, The RC column was tested under lateral displacement control while being exposed to a constant axial load of 855 kN, or around 10% of its axial compressive capacity.

The FEM was verified [20] by contrasting the generated results with the measured experimental data. Fig. 20 displays a comparison of the experimental and FEM findings for the lateral load and displacement of the RC column. In the

experimental test, the ultimate lateral load was 323 kN, which led to a lateral displacement in the column of 104.36 mm in the initial loading direction and 263.9 kN, which resulted in a displacement of 127 mm in the negative loading direction. The FEM model obtained results with errors of 0.83% and 6.2% for the lateral load and displacement in the initially loading direction, respectively, of 335 kN and 97.9 mm. The values of the load and displacement in the other loading direction were 269.42 kN and 131.38 mm, respectively, with errors of 2.1% and 3.12%. Flexural fractures first showed up 7.4 mm in the direction of the initial load on the tensile sides of the plastic hinge region. After achieving its maximum load, the concrete near the bottom of the RC foundation experienced significant crushing when the splitting of the concrete cover began, with an implemented displacement of 127 mm.

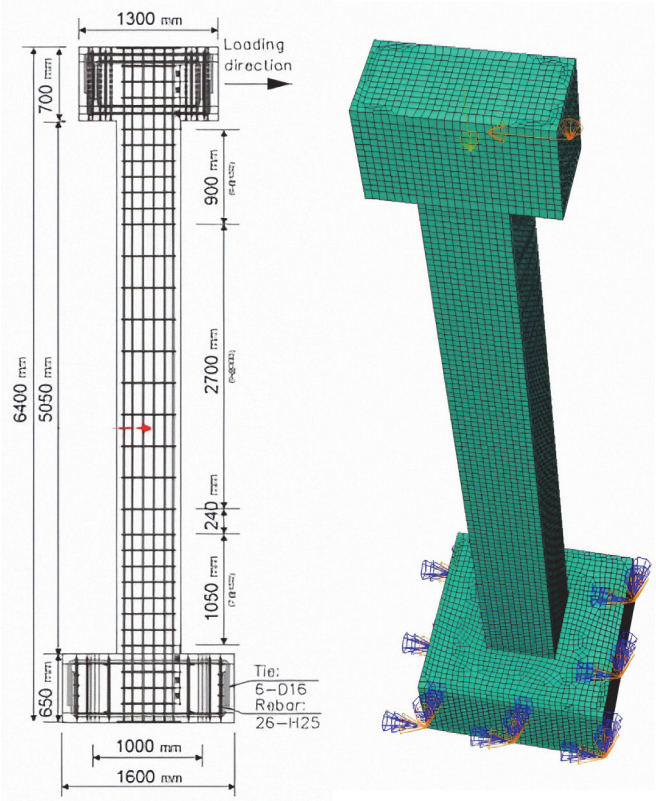

Figure 18. Details of RC column.

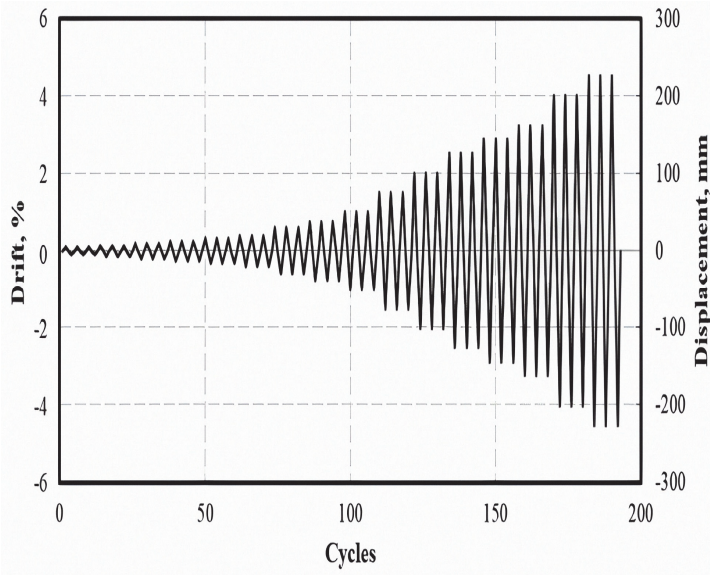

Figure 19. The loading protocol imposed on the column [21].

FE verification Model (RRC columns at cyclic loading)

A proposed 3-D model has the same geometry, material properties, boundary conditions, and loading pattern as the RRC column tested by Elghazouli [14]. The column's total length and span length were 1350 and 1000 mm, respectively, while the column had a diameter of 250 mm. Eight 12 mm-diameter steel bars and ten mm circular stirrups placed 100 mm apart served as longitudinal reinforcement for the column. As seen in Fig. 21, the column is composed of a rectangular base measuring 2100 x 600 x 400 mm and a rectangle top cap measuring 400 x 400 x 300 mm. The column has 60% rubberized concrete replacement. The column's concrete has a Fcu of 7.45 MPa. The longitudinal reinforcement's ultimate and yield strengths were 619 and 526 MPa, respectively. Transverse reinforcement's ultimate strength and yield were 603 MPa and 496 MPa, respectively. About 15% of the nominal axial capacity was applied to the column by the 20 kN axial load. the lateral cyclic displacements were applied in three cycles: 1.0 δy, 2.0 δy, and (2 + 2n) × δy. In each cycle, δy represents the predicted lateral yield deformation, and n can be any number between 1 and 4. In cases where the primary reinforcement was lifted at a lateral displacement δy of around 10 mm.

The FEM was verified by contrasting the resulting findings with the obtained experimental data. The experimental [14] and FEM results for the lateral load and displacement of the RRC column are shown in Fig. 22. In the experimental test, the highest lateral load was 54 kN at a lateral displacement of 35 mm in the initial loading direction, while in the negative loading direction, the maximum lateral load and displacement were 50 kN and 34.6 mm, respectively. The FEM model's lateral load and displacement in the original loading direction were 58 kN and 37.9 mm, respectively, with errors of 6.9% and 7.65%. The lateral load and displacement in the opposite loading direction were 54.6 kN and 35.2 mm, respectively, with errors of 8.4% and 1.7%.

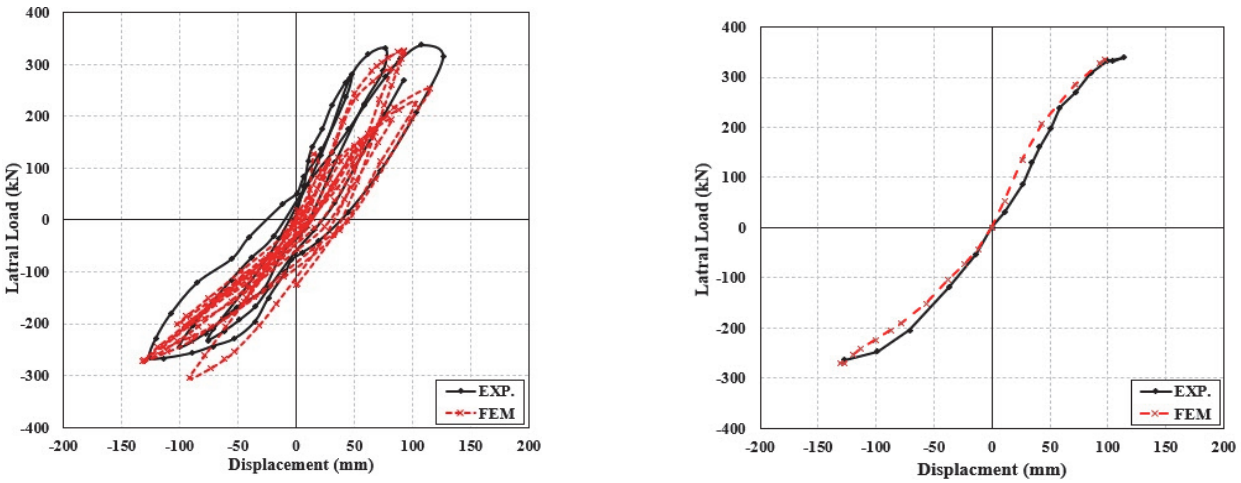

a- Load-displacement curves b- Backbone curve

Figure 20. Experimental [20] vs. FEM lateral load – lateral displacement of RC column.

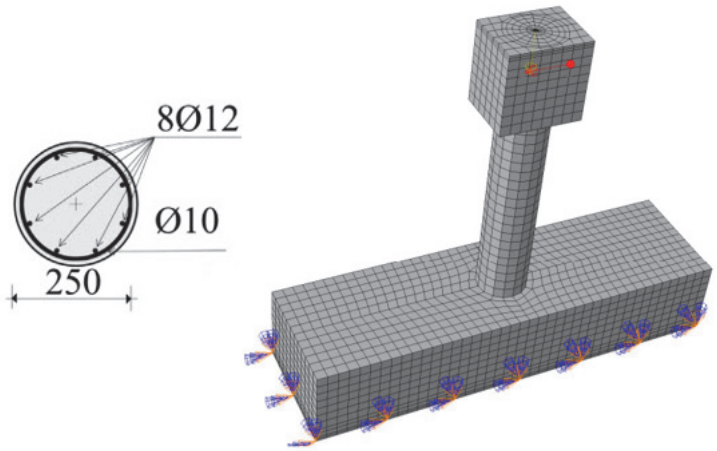

Figure 21. Details of RRC column.

Rubberized concrete columns' response at cyclic loading

In this research, the behavior of the experimentally tested columns when exposed to cyclic loads was investigated numerically using the FEM for square reinforced concrete columns with identical geometry, material characteristics, and boundary conditions. A reference point at the top of the column was used to apply a constant vertical load. Following the application of the axial load in the first stage, a horizontal displacement was applied via a reference point attached to the column head as part of a displacement control technique in the second stage (see Fig. 23). Square columns measuring 1.5 meters in height were subjected to an axial force of 190 kN, while columns measuring 1.8 meters in height were exposed to an axial load of 178 kN. This axial load is estimated to be about 10% of the axial compressive capacity of the columns in both cases. The lateral displacement of all columns was carried out in accordance with the loading protocol illustrated in Fig. 19 and detailed in ACI 374 [21]. A perfect bond between concrete and steel was considered, and no slip was observed in the experimental tests and FE verification model; thus, the interaction between reinforcing steel bars/stirrups and concrete was simulated using embedded constraints. According to Section 4-2, the concrete damage plasticity (CDP) model was used to determine the material properties of the steel bars and concrete for these columns.

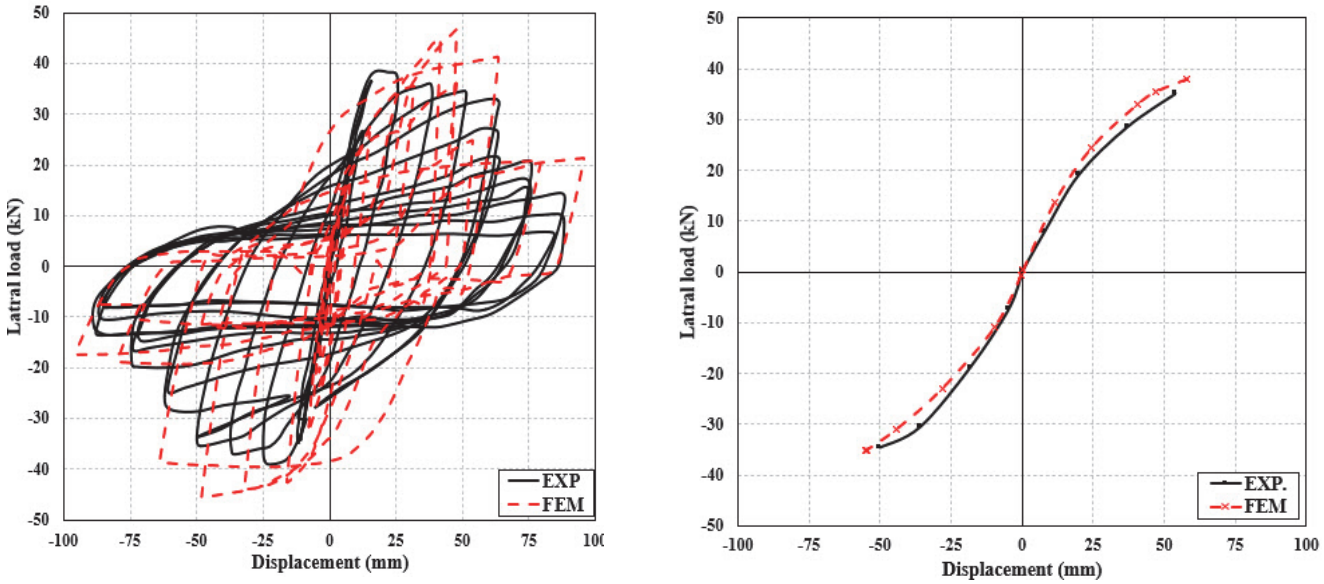

a- Load-displacement curves b- Backbone curve

Figure 22. Experimental [14] vs. FEM lateral load – lateral displacement of RC column.

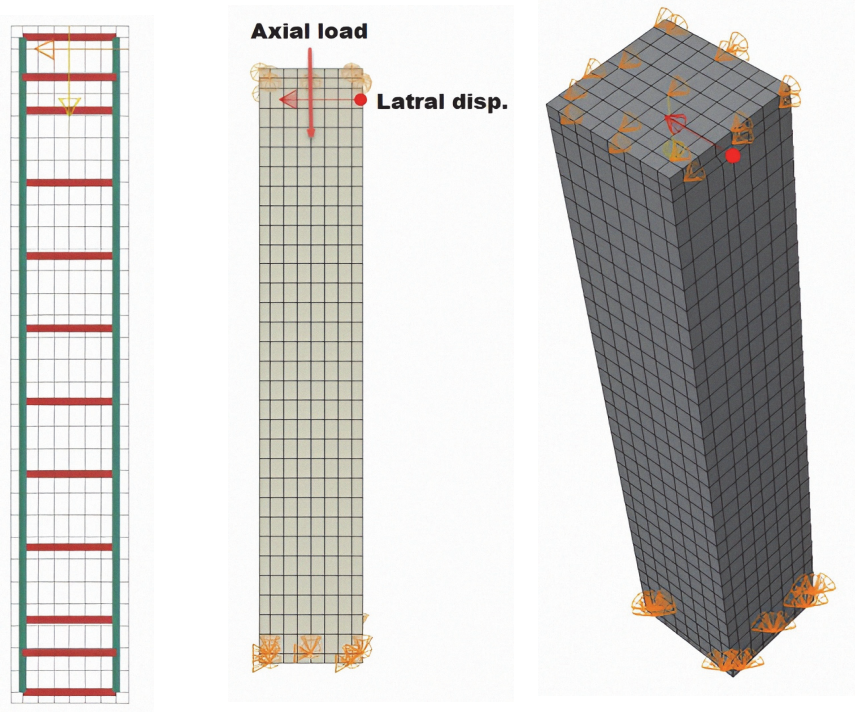

Figure 23. FE Model.

Hysteretic behavior and backbone curves

Figs. 24 and 25 show the relationship between the lateral force and the lateral column displacement for each column. The specimens exhibited almost a linear response up to the first give, after which persistent nonlinear symmetrical hysteretic loops appeared. Reinforced concrete columns with CR showed greater lateral displacement than reinforced concrete columns without CR, while the lateral load was greater in the RC columns without CR.

Table 5 illustrates the results of lateral displacement and lateral load for square columns in both positive (load direction) and negative directions. In a positive direction, the analysis showed that the ultimate lateral loads of reinforced square columns without CR are 5.6% and 6.7%, respectively, greater than those of RC columns with 10% and 15% CR replacement. In comparison to conventional RRC, square RRC columns with 10% and 15% have a 26.5% and 34.5% higher lateral

displacement, respectively. On the other negative side, the results indicate that the lateral load capacity of RC square columns without CR is greater than columns with 10% and 15% CR replacement by 34.21% and 38.3%, respectively. For the columns with a 1.5 m height, the lateral displacements of RRC square columns with 10% and 15% are greater than conventional RC columns by 24.5% and 29.03%, respectively, because the elastic characteristic of crumb rubber allows it to disperse energy It was noticed that the maximum lateral displacement of the RRC columns (R10% H1.8 S and R15% H1.8 S) is much higher than that of the normal concrete column (R0% H1.8 S) by 9.4% and 28.6%, respectively. The ultimate lateral load was reduced by 3.71% and 8.02% for square RRC columns with a height of 1.8 m as compared to RC columns without crump rubber. On the other negative side of loading, the values of lateral loads and lateral displacement for an RC column without CR were 23.73 kN and 99.61 mm, respectively. The reinforced concrete columns with 10% and 15% CR replacement exhibited lateral loads of 22.85 kN and lateral displacements of 103 mm and 106 mm, respectively. The findings provide quick insight into the impact of axial force and rubber composition on RC column behavior. The studies showed that rubberized reinforced concrete columns display delicate crushing behavior, leads to favorable energy dissipation and ductility properties when constract to normal RC columns.

Specimen code	Direction of initial loading			
	Positive direction		Negative direction	
	Load (kN)	Lateral displacement (mm)	Load (kN)	Lateral displacement (mm)
R0%H1.5S	49.3	101.15	45.5	102.3
R10%H1.5S	46.7	128	33.9	127.4
R15%H1.5S	46.2	136	32.8	132
R0%H1.8S	35	98.75	23.73	99.61
R10%H1.8S	33	108	22.85	103
R15%H1.8S	32	127	22	106

Table 5: A summary of the numerical results.

Displacement ductility

Using the following equation [22], the displacement ductility values (μ) of the columns were determined to compare the ductility of the columns.

$$\mu = \frac{\Delta_u}{\Delta_y} \tag{1}$$

The force-displacement hysteretic reactions illustrated in Figs. 24 and 25 were utilized to construct the bilinear approximation of the force-displacement envelopes, which obtained the Δ_u and Δ_y values. Table 6 displays the displacement ductility value of the RC columns that was computed. An increase in the ratio of crumb rubber from 0% to 10% led in an 80.47% increase in displacement ductility. Also, for columns 1.5 meters in height, the displacement ductility increased by 125.58% when the CR ratio was raised from 0% to 15%. However, the displacement ductility was increased by 38.95% and 85.79% for columns R10% H1.8 S and R15% H1.8 S compared with the control column R0% H1.8 S. Based on test results, the rubberized reinforced columns had a comparatively mild post-peak response, suggesting a more ductile reaction in contrast to normal RC. Fig. 26 shows the displacement ductility values of the square RC columns.

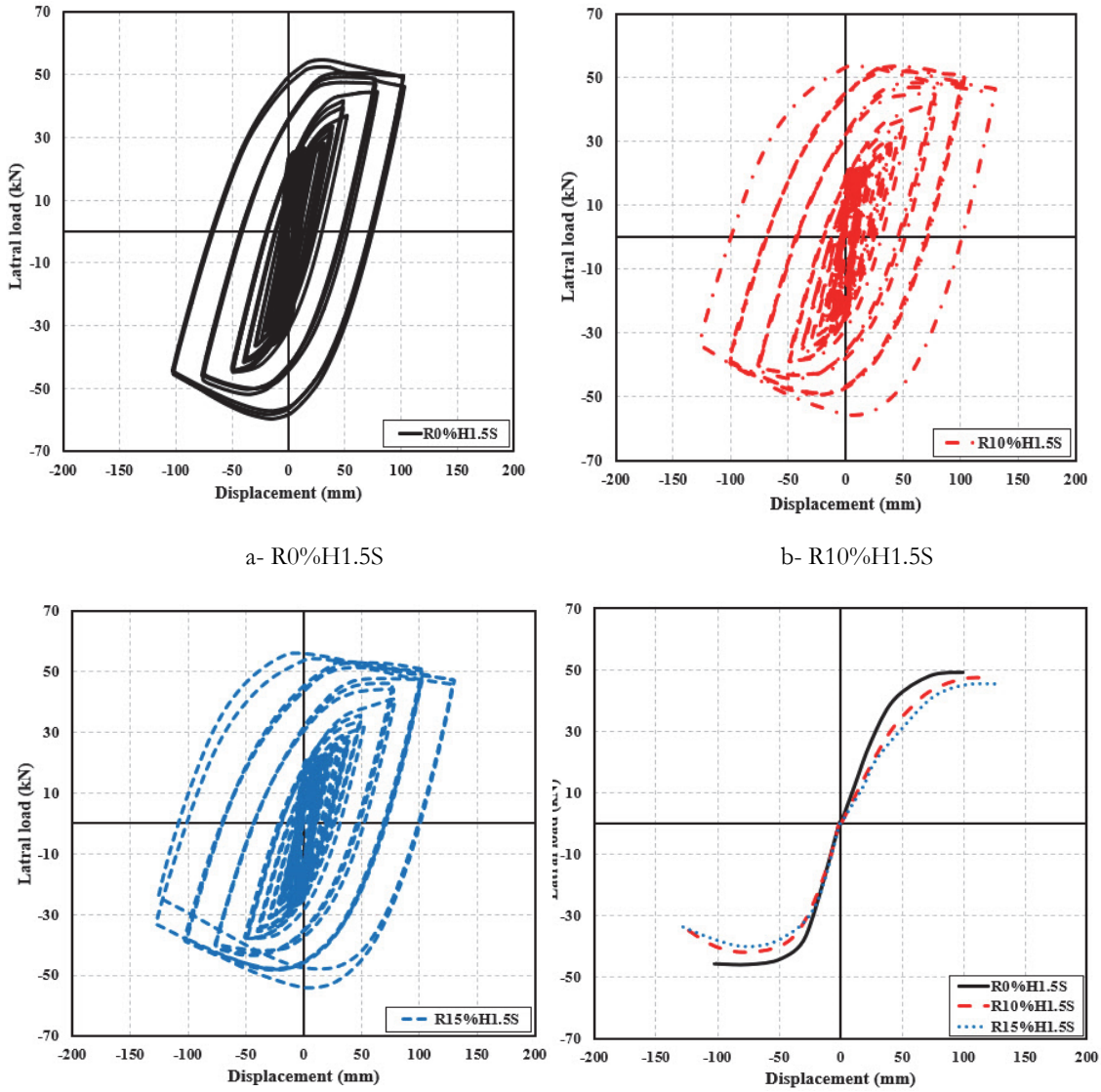

a- R0%H1.5S

b- R10%H1.5S

c- R15%H1.5S

d- Backbone curve

Figure 24: Square columns with 1.5 m height.

Specimen code	Yield displacement (mm)	Maximum displacement (mm)	Displacement ductility	Damping ratio
R0%H1.5S	47	101.15	2.15	12.95
R10%H1.5S	33	128	3.88	17.31
R15%H1.5S	28	136	4.85	18.65
R0%H1.8S	52	98.75	1.9	11.86
R10%H1.8S	41	108	2.64	14.61
R15%H1.8S	36	127	3.53	16.69

Table 6: Displacement ductility and damping ratio of columns.

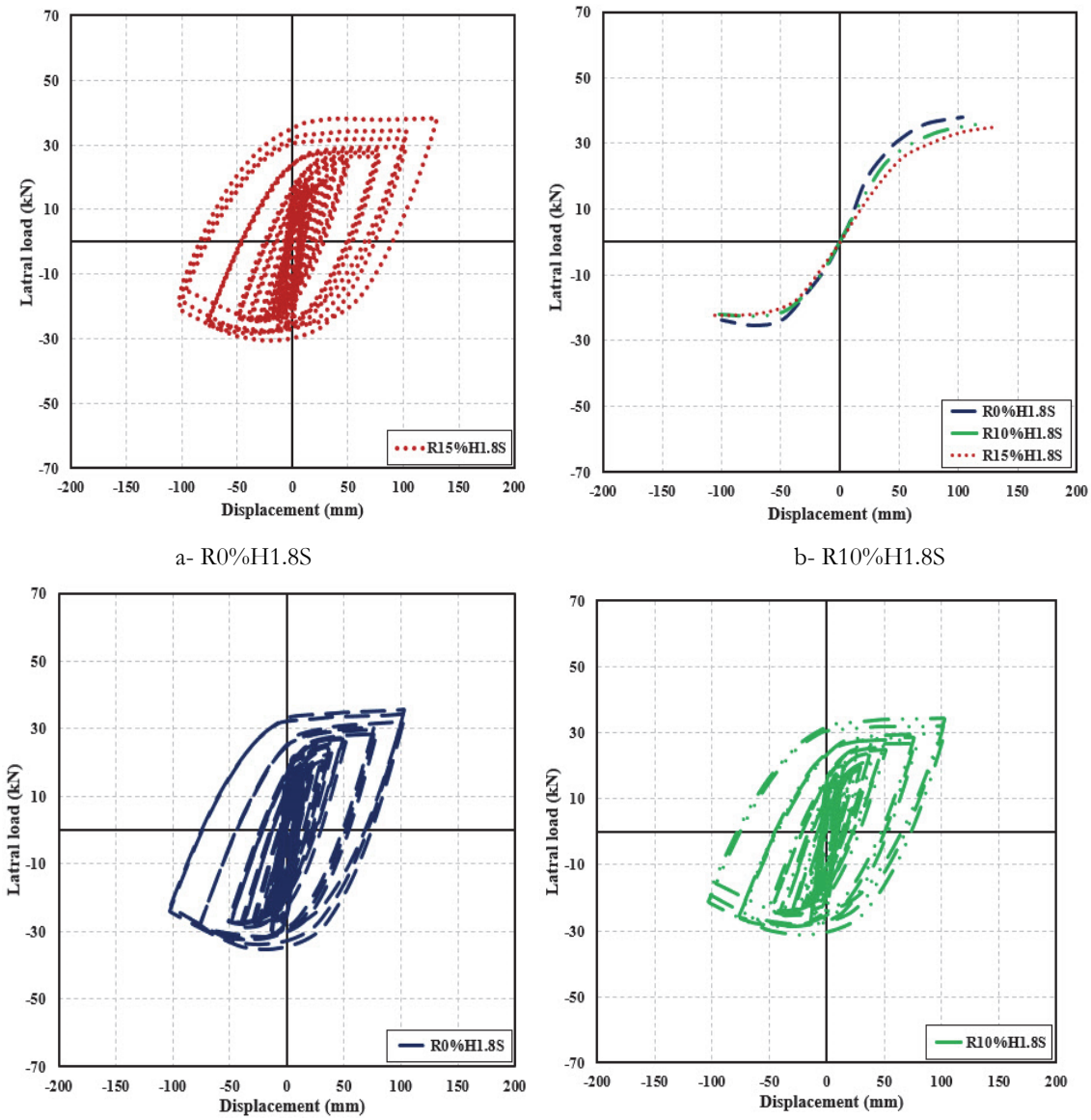

a- R0%H1.8S

b- R10%H1.8S

c- R15%H1.5S

d- Backbone curve

Figure 25. Square columns with 1.8 m height.

Equivalent viscous damping ratio

Structural damping is one of the most essential factors in determining how buildings will respond to seismic loads. To describe the damping behavior, equivalent viscous damping (ξ_{eq}), the most basic type of damping for numerical analysis, is usually employed. The ξ_{eq} can be calculated as

$$\xi_{eq} = \xi_s + \xi_{hys} \tag{2}$$

where ξ_{hys} is the hysteretic damping, which accounts for the fraction of the damping that happens through non-linear hysteretic behavior, and ξs is the initial elastic viscous damping; in this research, the word "elastic" is used to distinguish it from the equivalent viscous damping. ξ_s In addition to accounting for minor mistakes brought on by simplifications taken into consideration in the computation of ξ_{hys}, ξ_s also considers additional causes of damping, such as non-linearity in the foundation, radiation damping, and damping between structural and non-structural components.

To calculate equivalent viscous damping in relation to displacement ductility, many researchers created formulas. For instance, the comparable viscous damping was calculated as follows by Gulkan and Sozen [23]:

$$\xi_{eq} = 0.02 + 0.2\left(1 - \frac{1}{\sqrt{\mu}}\right) \tag{3}$$

Midorikawa et al. [24] modified the earlier equation by raising the initial damping in the elastic region and the factor 0.2 in front of the bracket to 0.25. The modified equation is as follows:

$$\xi_{eq} = 0.05 + 0.25\left(1 - \frac{1}{\sqrt{\mu}}\right) \tag{4}$$

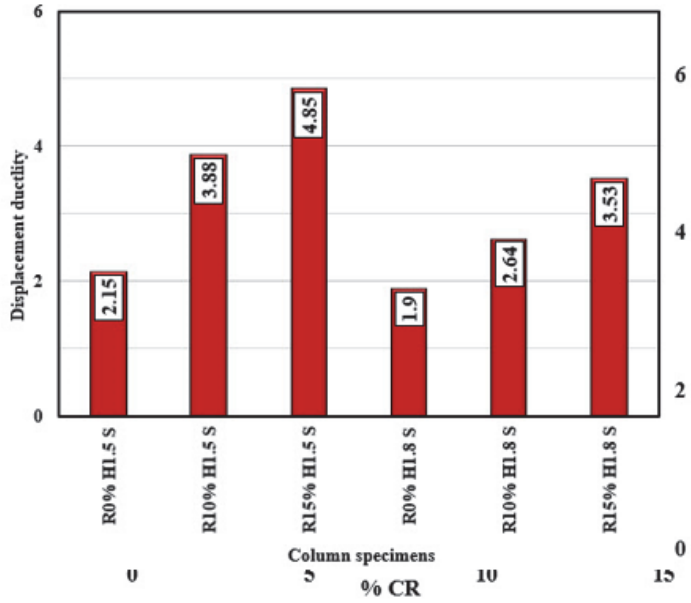

Figure 26. Displacement ductility values of columns

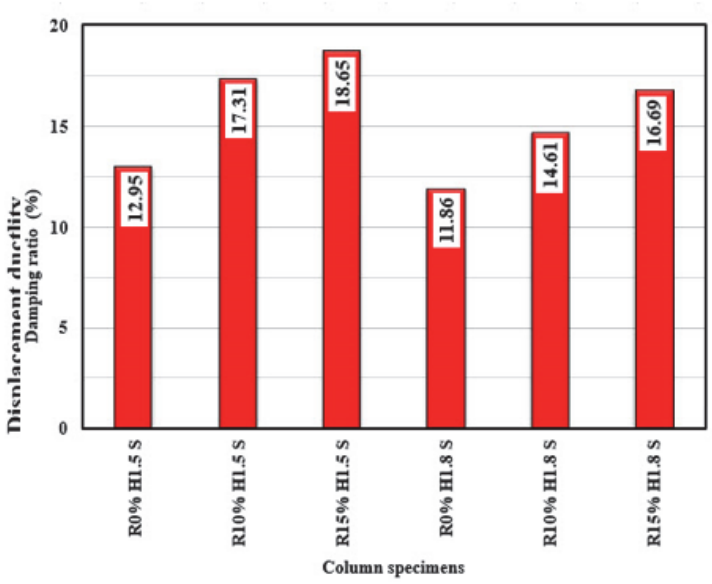

Figure 27. Damping Ratio values of columns.

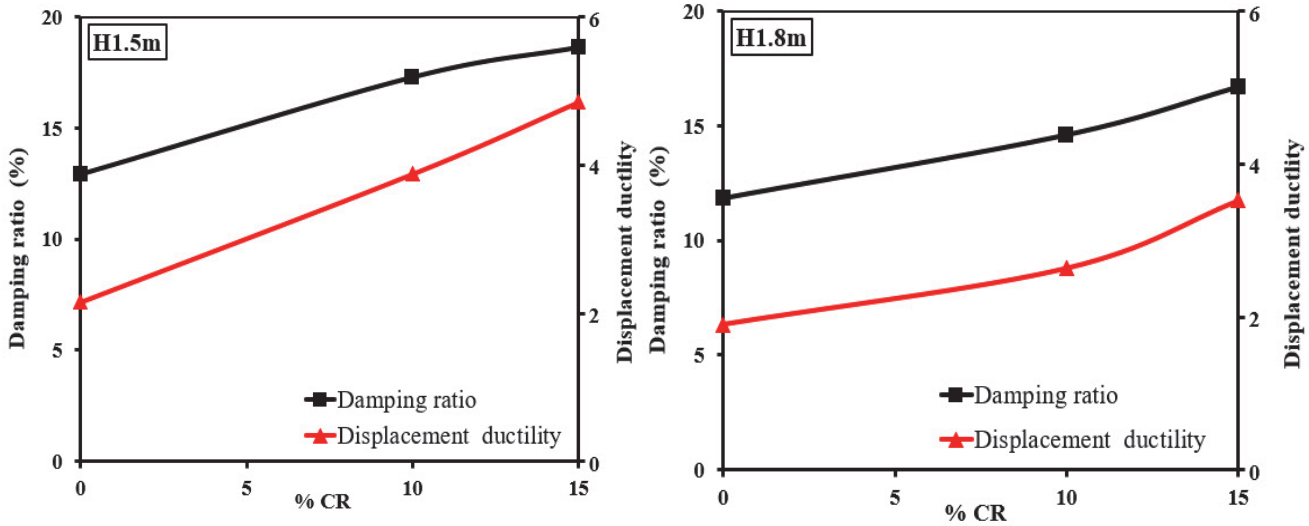

Figure 28. Effect of CR on displacement ductility and damping ratio of columns

In Fig. 27, the test data is displayed using Eq. 4. The figure shows how successfully the equation predicted the data's trend. However, it's systematically conservative. The equivalent viscous damping ratio improved by 33.67% when crumb rubber replacement was raised from 0% to 10%. At 15% replacement, the damping ratio rose to 44.02%. Additionally, employing rubberized concrete can help lessen the extent of damage by delaying the start of an earthquake's damage [25]. Rubberized concrete is more flexible than traditional concrete, so the amount of concrete cover splitting was delayed, and the amount of concrete cracking was minimal. The reason for these advantages is that rubberized concrete is more elastic than regular concrete. Rubberized concrete can be utilized as a green replacement for regular concrete in structural sections that are susceptible to the effects of cyclic loads.
As seen in Fig. 28, findings demonstrated that the use of crump rubber improve the displacement ductility and viscous damping ratio in reinforced concrete columns under cyclic loads [14].

CONCLUSIONS

This paper presents experimental and FEM to evaluate performance of RCC columns at axial and cyclic loads. Rubberized and conventional concrete were used to cast the tested reinforced concrete columns. The following conclusions might be drawn based on the study's findings:

Rubberized Reinforced Concrete Columns at Axial Loads (Experimental results)

- ✓ The value of compressive strength (Fcu) reduced by 18.33% and 26.5% when the fine aggregate was partially replaced by 10% and 15% CR, respectively, in contrast to concrete without CR.
- ✓ Adding a 10% and 15% CR to the fine aggregate resulted in an 18.5% and 25.5%, respectively, lower value compared to specimens without the CR.
- ✓ In general, the mechanical properties of crump rubber concrete reduced as the crump rubber content increased
- ✓ The rubberized reinforced concrete columns with 10% and 15% crump rubber showed a lower load capacity compared to RC columns without CR.
- ✓ For circular rubberized reinforced concrete columns with 10% CR and 1.5 m and 1.8 m height, the corresponding reduction in load capacity was 14.95% and 13.19%, respectively, over that of RC columns without CR. In the case of circular RRC columns with 1.5 m and 1.8 m height, the ratios of load capacity in columns with 15% CR decreased by 20.24% and 20%, respectively.
- ✓ The ductility index dropped when the crump rubber was used in reinforced concrete columns under axial loading.

Rubberized Reinforced Concrete Columns at cyclic Loading (Numerical results)

- ✓ The lateral displacement was significantly improved for rubberized reinforced concrete columns with 10% and 15% replacement of fine aggregates compared to columns without CR.
- ✓ The rubberized reinforced concrete columns with 10% and 15% CR indicated an increase in lateral displacement of 26.5% and 34.5% compared to the traditional RC column with a height of 1.5 m.
- ✓ The lateral displacement improved by 9.4% and 28.6%, respectively, when rubberized concrete columns with 10% and 15% replacement by 1.8 m in height were compared to columns without CR.
- ✓ The ultimate lateral loads of reinforced square columns with a height of 1.5 m without CR were 5.6% and 6.7%, respectively, greater than those of RC columns with 10% and 15% CR replacement.
- ✓ The ultimate lateral load was reduced by 3.71% and 8.02% for square RRC columns with a height of 1.8 m as compared to RC columns without crump rubber.
- ✓ The displacement ductility rose by 80.47% when the ratio of CR was raised from 0% to 10%. The displacement ductility of 1.5 m-height square columns rose by 125.58% when the CR ratio was raised from 0% to 15%.
- ✓ The square rubberized reinforced concrete columns with a 1.8 m height showed improvements in displacement ductility of 38.95% and 85.79% when the fine aggregates were replaced by 10% and 15% CR, respectively, compared to the columns without crump rubber.
- ✓ The rubberized reinforced concrete columns showed a more ductile reaction than the traditional reinforced concrete columns, as evidenced by their softer post-peak response.
- ✓ The equivalent viscous damping ratio was enhanced by 33.67% when increasing crumb rubber (CR) from 0% to 10%, and when crumb rubber (CR) replacement became 15%, the damping ratio increased to 44.02% for the columns with 1.5 m height.

- ✓ When 10% and 15% of the fine aggregates were replaced with CR in square RRC columns with a height of 1.8 m, the damping ratio rose by 23.19% and 40.73%, respectively.
- ✓ By using rubberized concrete, the damage from an earthquake may not occur as soon, which can assist to limit the amount of damage.

These conclusions showed that crump rubber can be employed in reinforced concrete columns without significantly affecting their final strength or deformability. However, crumb rubber concrete can delay and lessen the amount of damage produced by cyclic loads.

REFERENCES

[1] Chen, M., Si, H., Fan, X., Xuan, Y., Zhang, M. (2022). Dynamic compressive behavior of recycled tire steel fiber reinforced concrete. Constr. Build. Mater., 316 (3), pp. 22-35. DOI: 10.1016/j.conbuildmat.2021.125896.

[2] Pham, T.M., Elchalakani, M., Hao, H. (2018). Axial impact resistance of rubberized concrete with/without FRP confinement for sustainable roadside barriers. Int J Protect Struct. Revision. 10 (2), pp. 154-173. DOI: 10.1177/2041419618800771.

[3] Elchalakani, M. (2015). High strength rubberized concrete containing silica fume for the construction of sustainable roadside barriers. Structures., 1 (1), pp. 20-38. DOI: 10.1016/j.istruc.2014.06.001.

[4] Youssf, O., Hassanli, R., Mills, J.E. (2017). Mechanical performance of FRP-confined and unconfined crumb rubber concrete containing high rubber content. J Build Eng., 11 (1), pp. 115–126. DOI: 10.1016/j.jobe.2017.04.011.

[5] Ganesan, N., Bharati, R., Shashikala, A.P. (2013). Behavior of self-consolidating rubberized concrete beam-column joints. ACI Mater J., 110 (6) pp. 697–704. DOI: 10.14359/51686337.

[6] Son, K.S., Hajirasouliha, I., Pilakoutas, K. (2011). Strength and deformability of waste tire rubber-filled reinforced concrete columns. Constr. Build Mater., 25(1), 218-226. DOI: 10.1016/j.conbuildmat.2010.06.035.

[7] ACI(2014). Building Code Requirements for Structural Concrete and Commentary. Farmington Hills, MI, U.S.A: American Concrete Institute.

[8] AIK(2016). Korean Building Code and Commentary, KBC, Architectural Institute of Korea, Seoul, Korea.

[9] Liu, X., Li, Y. (2018). Experimental study of seismic behavior of partially corrosion-damaged reinforced concrete columns strengthened with FRP composites with large deformability. Constr. Build Mater., 191 (1), pp. 1071-1081. DOI: 10.1016/j.conbuildmat.2018.10.072.

[10] Zhang, P., Wang, Y., Mei, S., Liu, B., Xiao, J. (2020). Nonlinear damping properties of recycled aggregate concrete short columns under cyclic uniaxial compression. Constr. Build. Mater., 246 (1), pp. 71-83. DOI: 10.1016/j.conbuildmat.2020.118445.

[11] Zhou, X., Lu, D., Du, X., Wang, G., Meng, F. (2020). A 3D non-orthogonal plastic damage model for concrete. Compute. Methods Appl. Mech. Eng., 360 (3), pp. 112-126. DOI: 10.1016/j.cma.2019.112716.

[12] Mo, J., Zeng, L., Liu, Y., Ma, L., Liu, C., Xiang, S., (2020). Mechanical properties, and damping capacity of polypropylene fiber reinforced concrete modified by rubber powder. Constr. Build. Mater., 242 (1), pp. 118-232. DOI: 10.1016/j.conbuildmat.2020.118111.

[13] Bisht, K., Ramana, P. (2017). Evaluation of mechanical and durability properties of crumb rubber concrete. Constr. Build Mater., 155 (1), pp. 811-817. DOI: 10.1016/j.conbuildmat.2017.08.131.

[14] Elghazouli, A.Y., Bompa, D.V., Xu, B., Ruiz-Teran, A.M., Staffor, P.J. (2018). Performance of rubberised reinforced concrete members under cyclic loading. Engineering Structures., 166 (1), pp. 526–545. DOI: 10.1016/j.engstruct.2018.03.090.

[15] Sharaky, I.A., Mohamed, H. A., Torres, L., Emara, M. (2020). Flexural behavior of rubberized concrete beams strengthened in shear using welded wire mesh. Composite Structures., 247 (1), pp. 97-112. DOI: 10.1016/j.compstruct.2020.112485

[16] Xie, J.-H., Guo, Y.-C., Liu, L.-S., Xie, Z.-H. (2015). Compressive and flexural behaviors of a new steel-fiber-reinforced recycled aggregate concrete with crumb rubber. Constr. Build Mater., 79 (1), pp. 263-272. DOI: 10.1016/j.conbuildmat.2015.01.036.

[17] Ren, F., Mo, J., Wang, Q., Ming Ho, J. C. (2022). Crumb rubber as partial replacement for fine aggregate in concrete: An overview. Construction and Building Materials., 343 (6), pp. 22-49. DOI: 10.1016/j.conbuildmat.2022.128049.

[18] Dong, Q., Huang, B. and Shu, X., (2013). Rubber modified concrete improved by chemically active coating and silane coupling agent. Construction and Building Materials., 48 (1), pp. 116- 123. DOI: 10.1016/j.conbuildmat.2013.06.072.

[19] DSS (Dassault Systemes Simulia Corp) (2014). ABAQUS Analysis user's manual 6.14-2, DSS, Providence, RI, USA.

[20] Shin, D.-H., Kim, H.-J. (2020). Cyclic response of rectangular RC columns retrofitted by hybrid FRP sheets. Structures., 28 (2), pp. 697-712. DOI: 10.1016/j.istruc.2020.09.016.
[21] ACI (2013). Guide for Testing Reinforced Concrete Structural Elements under Slowly Applied Simulated Seismic Loads, ACI 374, American Concrete Institute, Farmington Hills, Michigan, U.S.A.
[22] Priestley, M.. Calvi, G., Kowalsky, M. (2007). Displacement-based Seismic Design of Structures. Pavia, IUSS Press, Italy. DOI: 10.1193/1.2932170.
[23] Gulkan, P., and Sozen, M. A. (1974). Inelastic responses of reinforced concrete structures to earthquake motions. J. Am. Concr. Inst., 71 (12), pp. 604 - 610. DOI: 10.14359/7110.
[24] Midorikawa, M., Hiraishi, H., Okawa, I., Iiba, M., Teshigawara, M., and Isoda, H. (2000). Development of seismic performance evaluation procedures in Building Code of Japan. Proc., 12th World Conf. on Earthquake Engineering, Silverstream, New Zealand.
[25] Kalman Sipos, T., Jelec, K. and Milicevic, I. (2023). Seismic performance of rubberized concrete in structural applications. Proceedings of the 2nd Croatian Conference on Earthquake Engineering., 2CroCEE. DOI: 10.5592/CO/2CroCEE.2023.119.

NOMENCLATURE

Fcu	Compressive strength
Ftu	Tensile strength
Pu	Ultimate load
Δy	Yield displacement
Δu	Ultimate displacement
DI	Ductility index
λ	Buckling coefficient
μ	Displacement ductility
ξeq	Equivalent viscous damping
ξs	Initial elastic viscous damping
ξhys	Hysteretic viscous damping